

<https://doi.org/10.48047/AFJBS.6.13.2024.3787-3811>



African Journal of Biological Sciences

Journal homepage: <http://www.afjbs.com>



Research Paper

Open Access

Dental Image Classification using NAG optimization with EfficientNet-B0 for detecting Dental Caries

¹S. SRIVIDHYA SANTHI

Research Scholar, Department of Computer Applications, Email id: srividhya.mca@drmgrdu.ac.in

²Dr. R. SHOBA RANI

Professor, Department of Computer Science and Engineering

^{1,2}Dr.MGR Educational and Research Institute

Maduravoyal, Chennai-600 095, Email id: shobarani.cse@drmgrdu.ac.in

Article History

Volume 6, Issue 13, 2024

Received: 18 June 2024

Accepted: 02 July 2024

doi:

10.48047/AFJBS.6.13.2024.3787-3811

Abstract: One of the most prevalent dental diseases globally is dental caries. It is the medical name for the widespread condition known as tooth decay or cavities. People of all ages are susceptible to dental decay these days. Immediate diagnosis is crucial for effective treatment to prevent the patient from suffering from potentially life-threatening consequences. Dental caries, also referred to as tooth decay, is a widespread chronic condition that occurs when tooth enamel breaks down. The acid produced by the bacteria in the mouth causes tooth decay by eroding the enamel and eventually leaving a tiny hole in the tooth. If left untreated, oral illnesses may cause a cascade of complications, including receding gums, cavities, tooth loss, and even bone loss. The dentist greatly benefits from X-ray scans. To help with patient diagnosis and treatment, they use these images. On the other hand, not even a trained eye can easily decipher X-ray images. Many in the medical industry are interested in tooth recognition and teeth separation from X-ray images due to its practical applications. The objective here is to categorize illness rather than the progression through its phases, but there may be many stages of dental caries. In this study, we classified dental images to identify caries using Nesterov Accelerated Gradient (NAG) optimization using EfficientNet-B0. For the purpose of dental carrier segmentation, we used an improved Unet with ANN. When we compared our approach to others, the findings showed that it was more accurate and performed better.

Keyword: Dental Image, Segmentation, Classification, ANN, U-Net, NAG optimization, EfficientNet-B0.

I. INTRODUCTION

Half of the global population may be living with an oral illness at any one time, and 2.3 billion individuals are permanently tooth-deficient due to cavities [1]. Poor oral hygiene and other oral health issues, such dental caries and its sequelae, are frequent and may worsen due to factors like poverty, yet just 4.6% of total healthcare expenditure is expected to be devoted to oral healthcare worldwide. Cavities in teeth occur when the oral cavity's microbiological flora changes and acid

production increases, leading to the pathological deterioration of tooth tissue. Several inherited deficiencies, systemic diseases, and favored behaviors influence caries development. When treating incipient carious lesions, practitioners typically choose conservative methods that adhere to minimally invasive dental norms, while patients choose to disregard them. Therefore, there is a significant risk of misdiagnosis and mismanagement, particularly among younger practitioners who are doing visual and radiographic examinations [2]. The classic method for diagnosing caries lesions was a mix of visual-tactile detection assessment and bitewing radiography. In addition, bitewing radiography has been used for quite some time by dentists to uncover proximal caries that would otherwise go undetected during a thorough clinical visual examination. After the canine has lost its distal surface and before the farthest back molar has fully erupted, a posterior bitewing examination should take aimage of each tooth's crown. Radiographic examination is known to be an important tool for diagnosing caries lesions on the proximal surfaces of teeth [3]. Because of this, the diagnostic and therapeutic outcomes are highly dependent on the reading expert's skill and the available technology.

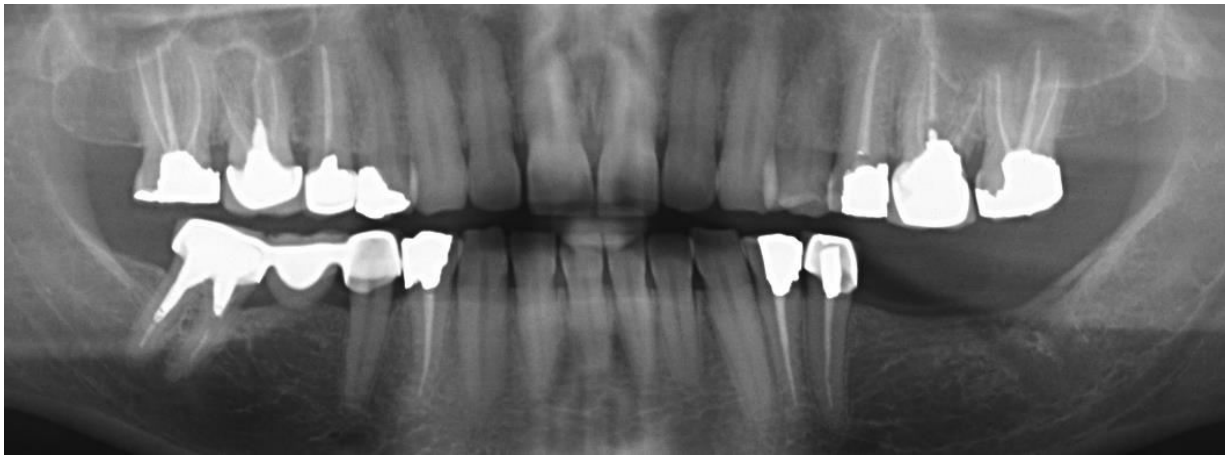


Figure 1. Sample dental image with tooth carrier

Chemical reactions involving fermentable carbs and acid-producing bacteria only ever lead to dental caries. The demineralization of enamel and dentin begins in tiny cracks and along the smooth surface of teeth due to an important acid included in dental plaque. The first sign of tooth disease or cavities is the emergence of a white spot. Permitting the demineralization process to proceed causes the little white spot to become pitted, and eventually, cavities, which are very small holes in the tooth surface. Young children (those aged 5 to 10), adolescents, and older children are the demographics most likely to experience this. But that white spot, or signs of caries, will surely be present in every tooth-bearing adult. Without treatment, the decay or cavities in that area will continue to build up, eventually leading to tooth loss, discomfort, and other dental problems [4].

Research in the area of medical imaging is seeing rapid growth within the healthcare arena. Medical imaging is crucial for three main reasons: early illness detection, diagnosis, and therapy. Examples of such images include x-rays, CT scans, MRIs, ultrasounds, and so on [5]. Radiologists often use radiography as a tool to aid in the evaluation of oral health and the detection of dental disorders such proximal dental caries. Radiographs are used to identify caries lesions on proximal tooth surfaces since these areas are difficult to reach or see directly. Bitewing, Panoramic, and Periapical x-rays are only a few examples of the several dental x-ray forms that capture various dental anatomy views [6]. Dentists use a variety of x-ray detectors. The two most common x-ray images used to identify dental problems are

orthopantomograms (OPGs) and radiovisiography (RVGs). An OPG image may take aimage of your upper and lower teeth simultaneously. Conversely, a single tooth may be diagnosed using RVG x-ray images. The interpretation and categorization of RVG x-ray images is challenging even for experienced radiologists due to irregularities such as size, angle, form, shadow, etc. In order to deduce the cause of these x-ray artifacts, one needs domain knowledge, competence, and experience. It takes a lot of time and energy to complete this procedure. Machines are capable of doing such operations with ease, speed, and precision [7].

Classification of teeth is the main application of dental image segmentation. A concealed anomaly in the tooth structure, such as a cavity, caries, etc., may be located using this. The most intriguing use of forensic identification is in the scientific and technological realms. As an example, forensic dentists use morphology in restoration to determine which victims were involved in a calamity. While biometric information is often inaccessible during a postmortem or within a few days after a person's death, dental structures may be recovered. Age estimate, plaque analysis, and similar applications also make advantage of this. A lot of people are interested in dental segmentation [8].

When applied to a variety of real-world challenges, deep learning becomes indispensable. At this time, many issues can be effectively addressed by using neural networks and deep learning. It simplifies the process of delivering the outcomes. Activation function, parameter initialization, learning rate, and other factors allow machines to effectively train on large datasets. When training a dataset on a computer, there are several aspects to consider. Higher levels of accuracy were achieved by efficient training on a dataset. In addition, there are a lot of factors to consider when an algorithm is prepared to execute. One of the key components of deep learning is the dataset, which contains the actual data required to train the model. Images, text, music, video, and so on might all make up a dataset [9].

With access to such a large dataset, CNNs show great promise for use in clinical assessment and diagnosis. Academics in the field of deep learning have just recently started to look at this possibility in the field of dental radiography. Panoramic radiographs, bitewing radiographs, and periapical radiographs have all found useful applications for convolutional neural networks (CNNs), such as diagnosing periodontal bone loss, detecting carious lesions, and apical lesions, respectively. Google News (CNNs) in dental radiology is explored in detail [10]. Agricultural and traffic detection are only two of the many image categorization sectors that have made use of CNN. Many significant and reliable architectures, such as AlexNet, VGG16, VGG19, ResNet50, and InceptionV3, were released with the fast advancements in GPU cards and the growing quantity of datasets. One method of deep learning is transfer learning, which enables the use of prior model training data for new tasks. There are several benefits to transfer learning. Transfer learning is especially helpful when the size of the new training dataset is modest; it saves time by beginning from the end of the most recent training instead of training the new model from scratch; it extends the information it obtained from prior models. The domains of computer vision, audio classification, and natural language processing have all benefited greatly from transfer learning [11]. In this study, we classified dental images to identify caries using Nesterov Accelerated Gradient (NAG) optimization using EfficientNet-B0.

II. RELATED WORKS

In recent years, deep learning algorithms have shown promise in the identification and diagnosis of dental diseases. Thanks to advancements in GPUs, faster CPUs, huge data sets, and multi-

layer artificial neural networks, deep learning has become a profitable field. Here, we compiled information from our study on several methods for detecting dental diseases.

Using dental X-ray images, Ivane Delos Santos Chen et al. [12] demonstrated a successful way to detect periodontitis and dental caries at the same time. Utilizing image processing techniques such as bilateral filtering and contrast-limited adaptive histogram equalization, as well as the EfficientNet-B0 model, the approach employs YOLOv7 for tooth detection. Several performance measures showed that the suggested strategy was effective. Dental professionals may benefit from their deep learning-based approach, which has shown encouraging capabilities, in identifying dental cavities and periodontitis.

According to EidAlbalawi et al. [13], a new standard has been established by their pioneering work, which includes a very effective deep learning model for the automated identification of Oral Squamous Cell Carcinoma (OSCC) from histopathology images. The algorithm deftly differentiates between "Normal" and "OSCC" tissues, maintaining accuracy, precision, and recall rates over 99% throughout. This has great promise for revolutionizing diagnostic capacities and is of great importance in the therapeutic, diagnostic, and research spheres. Not only does their success pave the way for improved patient outcomes, but it also allows for more prompt interventions and individualized treatment plans.

The accuracy of classifying segmented dental images as ideal edentulous, partially compromised edentulous, and substantially compromised edentulous cases was trained and validated by G. Divya Deepak et al. [14] using the Deep Network Designer module. This is crucial for improving treatment quality and processing time for the patient, leading to better health-care solutions. The three pretrained DNNs used in this study are EfficientNet-b0, ResNet-50, and SqueezeNet. After comparing EfficientNet-b0 to ResNet-50 and squeezeNet, a pretrained neural network, we find that EfficientNet-b0 attained the best accuracy of 98%.

The use of the transfer learning process to identify susceptible human teeth might greatly alleviate the physical labor required by dentists, as noted by FammeAkterMeem et al. [15]. They employ X-ray images for identification in their process by comparing them to the data that has been taught before. Nevertheless, if the system is capable of doing it automatically, it implies that the machine can provide the desired outcome. This will lead to further automation and, eventually, the implementation of mechanical instruments to rapidly discover reports. While densenet201 achieves a respectable 98% accuracy rate, inceptionV3 operates at a more efficient 93% rate; a comparison of the two methods' run times reveals that inceptionV3 requires less time.

Artificial intelligence has the ability to improve remote oral lesion detection, as highlighted by ViduniLiyanaage et al. [16]. This might be especially helpful for communities who do not have easy access to dentists. Using Deep Convolutional Neural Networks MobileNetV3 and EfficientNetV2, they were able to categorize and detect a variety of oral lesions in their proof-of-concept research. Additional refining is needed to improve the models' capacity to identify non-neoplastic lesions, while they showed promise in differentiating between benign neoplasms and premalignant/malignant lesions.

Using deep learning and Demirjian's technique as its foundation, Seung-Hwan Ong et al. [17] presented a completely automated system for dental development staging. There are three steps to the suggested process: identification, separation, and categorization. At each step, we tested the models' efficacy using YOLOv5, U-Net, and EfficientNet; we found that they performed well across a range of measures. With a detection model mAP of 0.995 and a segmentation model accuracy of 0.978, the detection and segmentation operations demonstrated encouraging

outcomes. The Incisor, Canine, Premolar, and Molar models of the classification model obtained F1 scores of 69.23, 80.67, 84.97, and 90.81, respectively.

AradhanaSoni et al. [18] Oral squamous cell cancer (OSCC) may now be automatically diagnosed using DL approaches that are as good as, if not better than, those of human experts in the field. Oral histopathology images were automatically classified as normal or malignant using better DL-CNN models in their research. Their study developed a CNN model that is based on EfficientNetB0. The candidate models were fine-tuned according to their architecture, and a DL-CNN model with the recommended extra layers was constructed for efficient OSCC detection. The EfficientNetB0 DL-CNN model outperformed the other modified models with an accuracy of 86.66%.

NRMSProp was suggested by RehamElshamy et al. [19] as an improved variant of the Adaptive optimizer. With the Nesterov technique's efficiency paired with the RMSProp optimizer, it pushes the RMSProp method to the next level. The Adam, RMSProp, and NRMSProp optimizers are tested on the Fashion-MNIST, CIFAR-10, and Tiny-ImageNet datasets in order to evaluate the suggested method NRMSProp. After running NRMSProp through its paces on several datasets, we compare its performance to that of Adam and RMSProp optimizers using APR, F1-score, the confusion matrix, and precision and recall. The NRMSProp demonstrated rapid convergence and good accuracy across all metrics without significantly adding complexity, according to the findings.

A machine learning approach was presented by Omid HalimiMilani et al. [20] that correctly classifies the orthopantomogram (OPG) phases of the lower third molars' development. The method's 83.7% accuracy rate is achieved by using a new convolutional neural network (CNN) that incorporates two trainable preprocessing filters into the pre-trained EfficientNet architecture. With a score of 83.7%, EfficientNet outperformed the competition, according to their results.

In a study by Daniela Lopez-Betancur et al. [21], twelve optimization algorithms were tested on an AlexNet CNN and an MLR. The objective was to determine how many black points, representing suspended solids, would be distributed randomly on a white background image. This would represent the total amount of suspended solids in the liquid sample. The objective was to compare how well various optimizers performed in multiple linear regression and image classification tasks including suspended particles in liquid samples. Thus, nine classes ranging from 0 to 50,176 black pixels per image were used to train AlexNet and the MLR. To verify the models, eight further classes were added, which were not used during training, and they ranged from 3136 to 47,040 black pixels per image. The results proved that the features of each optimizer's dataset impact their performance. Adam, AdamW, and NAdam were determined to have the three degraded optimizers' performances. According to the results, the top five optimizers were ASGD, Rprop, Adamax, and Adagrad.

According to Kelwin Fernandez et al. [22], SVMs failed on both tasks when compared to Classic Multilayer Perceptrons trained using the error backpropagation approach. Teeth and palates were better distinguished with the use of image filtering, adaptive curve fitting, and augmentation. The technology they developed could handle differences in patient anatomy, image mouth size, and viewing angle with ease. It also succeeded in resolving common issues with image processing systems, including lighting and quality variations.

To classify conditions and number tooth positions, SZU-YIN LIN et al. [23] built a DPR classification system using convolutional neural networks (CNNs), image pre-processing, and data augmentation. Dental diagnostic conditions might be categorized using their technique, which would be helpful for both professional dentists and medical personnel. In order to

complete the necessary dental follow-up treatments for patients, dentists might use their medical diagnostic decision support system. Numbering the positions of the teeth and classifying the conditions were the two parts of the experiment. With the use of their investigation, we can now automatically categorize individual tooth images in the DPR and ascertain their present state. As a result, the dental staff will have less work to do and DPR processing will be more efficient, allowing them to quickly learn about patients' oral health and provide timely follow-up care. Classification accuracy using dental position numbers exceeded 90% for 25 out of 32 teeth.

Summary:

- Some techniques may be used in clinical practice and forensic odontology to aid in the quick and impartial assessment of dental maturity and age estimate.
- There are ways to extract single tooth from an image with higher precision and thoroughness; this might help lower the rate of noise and recognition-related errors.
- Machine learning techniques, which have strong ties to computer statistics, are used to empower computers to learn on their own from data and carry out certain activities, such predictive analytics. Deep Learning (DL) is an area of Machine Learning (ML) that uses ANNs to model the brain's natural neural network architecture.

III. PROPOSED METHOD

Tooth decay affects individuals of all ages these days. The patient risks developing life-threatening consequences if the condition is not diagnosed and treated promptly. Tooth decay detection will help the dentist find caries early and will also remove the limitations of previous diagnostic methods. Infections of the mouth or gums are becoming a global epidemic. The present evaluation notes that people use numerous dangerous goods in their everyday life, which is the major reason of worry. In all industrialized nations, the affection rate for school-aged children is 60-90% and for adults it is near to 100% [3]. A public database is used to gather the dental X-ray images. Start training the model once dental x-ray images have been preprocessed. For segmentation, we used ANN with U-Net. For image classification, EfficientNetb0 makes advantage of Nesterov Accelerated Gradient (NAG) optimization, as seen in figure 1. Lastly, the results acquired from the deep learning model are compared to the old approach and analyzed using metrics such as accuracy, precision, sensitivity, and F1_score.

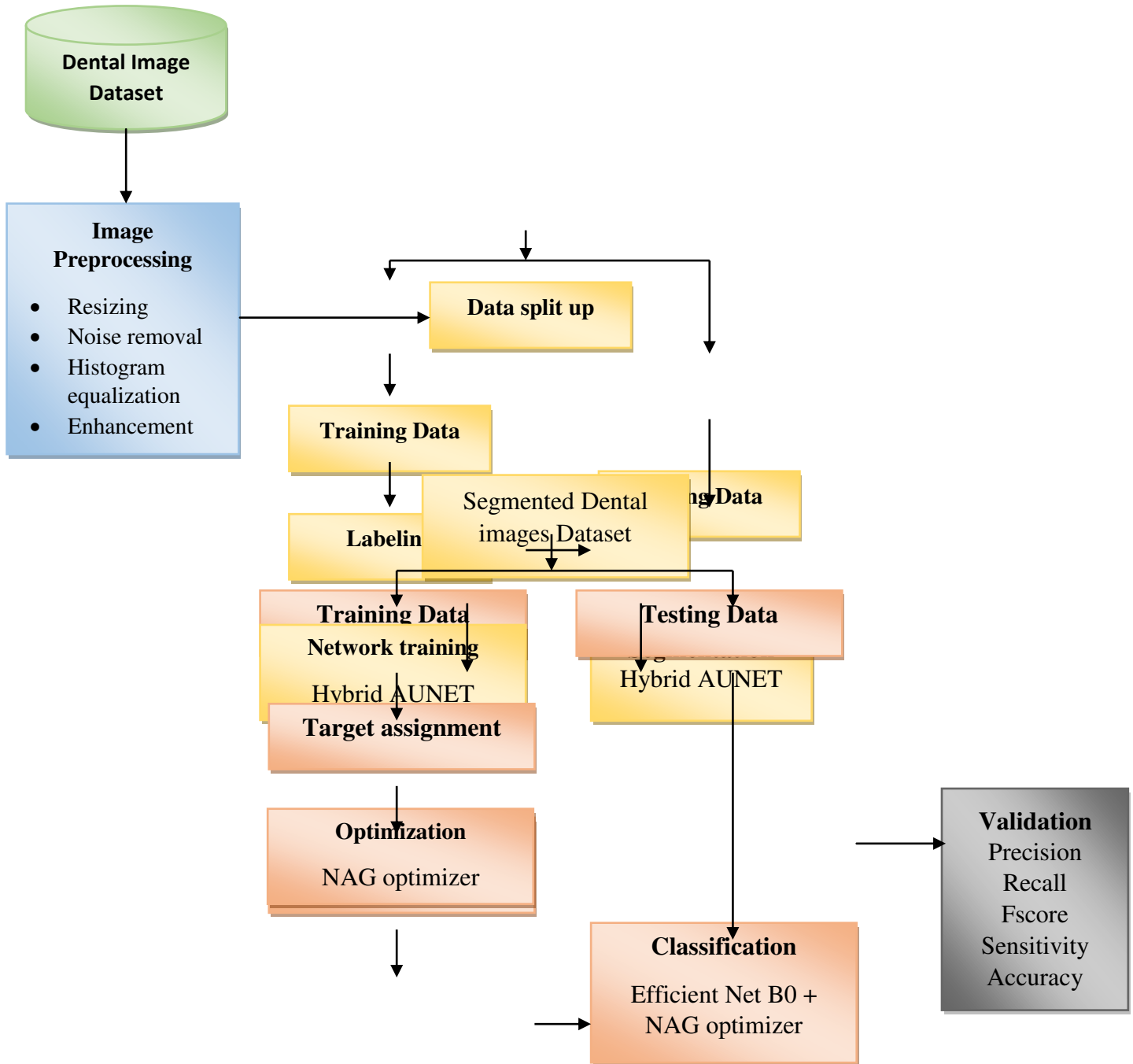


Figure 2. Block Diagram of proposed model

i) Dataset

There are a total of 534 abnormal images and 100 normal images in the dataset used for classification in this study. Training and testing use 70% of the dataset, while the other 30% is reserved for analysis. For the training process, we have five classes: I, II, III, IV, and V. Each class has 92, 85, 87, 27 afflicted images and 20 normal images. In addition to 10 normal dent imagegraphs for each class, there are 39,37,37,12,35 impacted images for testing purposes.

ii) Preprocessing

Transfer learning methods divide the preprocessed images into two sets, one for training and one for testing. Eighty images were used for training and forty for testing, for a total of 120 images included in the study. Based on the results, it seems that the test data includes both good and bad dental images. We may prepare the images for training in the transfer learning module when we finish the train test splitting [15].

iii) Image Augmentation

When the training set is larger, the network performs better. If you have an image dataset and want to make a lot of copies, all you have to do is rotate, flip, zoom, or crop the original. These changes improve the network's performance and make it better at avoiding overfitting. To solve this problem, we first flip, rotate, zoom, and shift the source images. According to reference 11, the images were rotated 180 degrees, horizontally and vertically flipped at random, subjected to a shifting range of 25%, and zoomed in at 40%.

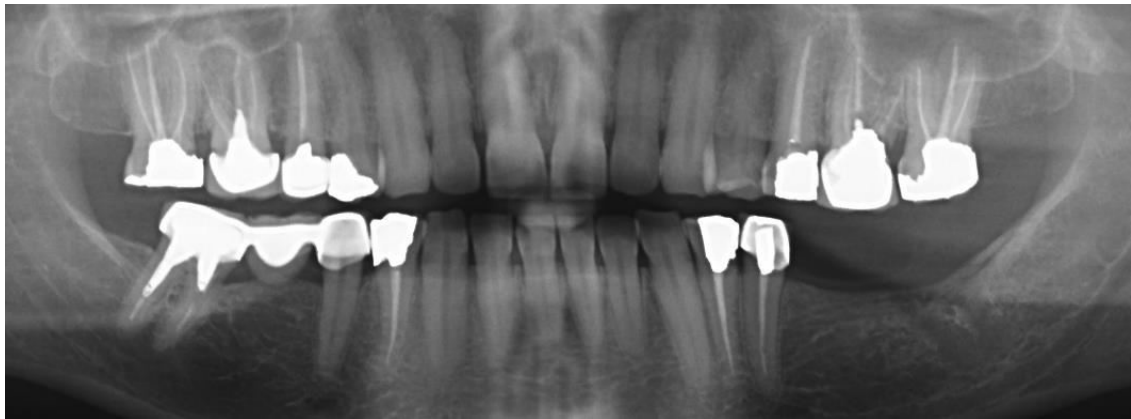


Figure 3. Preprocessed image

Resize: Data augmentation image resizing also requires checking whether image IDs are within the range; otherwise, image identifiers can be outside the display. Hence, the values used for this research likewise fall within the range of 0.1 to 0.9, which is necessary to prevent the target objects from being generated beyond the image's resolution. The range $[1-\text{value}, 1+\text{value}]$ is used for float values when zooming or resizing. Any value between 0.1 and 0.9 indicates that the zoom ratio is being utilized in the resizing process. An augmented image with a zoom ratio of 70% to 130% of the original image is produced when the parameter value is set to 0.3 [23].

iv) Segmentation using ANN and U-Net

Artificial Neural Network (ANN) and Neural Network (NN) are interchangeable terms. The operation of neurons in the human nervous system is the basis for Neural Networks. An activation function is applied to a fixed number of nodes in each layer. Each node has a complete connection to the layer below it. Assisting these linkages are weights. The output of each neuron is sent to the next layer once it has done the dot product of its input and weight [7] [24].

Using the decoder network to encode and decode the feature is key to the U-Net concept. It aids in retrieving spatial information that was lost during the max pooling procedure and provides data from the encoder to the decoder route. It is possible to decrease the amount of superfluous data sent across the skip link by including an attention gate into it [8].

For the purpose of dental carrier segmentation, an improved Unet with ANN is used. When applied to image segmentation and similar tasks, the UNet architecture's combination with an ANN produces a potent model. Image segmentation is one area where UNet, an architecture of convolutional neural networks (CNNs), has shown to be quite successful. The use of an ANN improves its performance on a wide range of tasks, including image categorization and object recognition.

Hybrid Model details as follows

- Integrating the UNet's output into the ANN for further processing is one way to integrate the UNet and ANN.
- As an example, the UNet's segmented areas may be fed into the ANN's classification process.
- The combined model can be represented as follows:

$$P(Y) = C(D(E(X))) \quad (1)$$

X is the input image; E is the encoder part of the Unet; D is the decoder part of the UNet.

C is the ANN for classification.

The input image is processed by the UNet, which then extracts features. The decoder then creates segmented areas, which are then subjected to further processing or classification by the ANN.



Figure 4. Segmented dental image

v) **Feature Extractor**

The feature extractor is a pre-trained model that has been trained on a large dataset. The custom network is then fed these properties as inputs. Using the massive dataset, the pre-trained model picks up on the most fundamental, low-level properties.

One method that was used for feature extraction was the GLCM algorithm. The feature extraction process yields values for characteristics including GLCM contrast, energy, correlation, and homogeneity. These features are quantized with values of 8, 16, and 32, and their direction cooccurrence is 0, 45, 90, or 135 degrees. Pixel distance (d) is 100 or 200.

The features extraction step may be executed using two MATLAB routines. The graycomatrix is used to create a GLCM matrix, and the graycoprops are used to access the features of the GLCM matrix. Quantization, a co-occurrence matrix, symmetry, and normalizing are the parameters that make up the graycomatrix function. In the meanwhile, the four qualities that made up graycoprops' function were homogeneity, energy, GLCM contrast, and correlation. Three quantization values—8, 16, and 32—were employed in this investigation. In order to speed up

the computing process, quantization is used to decrease the amount of computations. Making a co-occurrence matrix using adjacent pixel intensity values at one level, distance from other pixels at another level (d), and a certain orientation angle (θ) is the next step after finding the quantization values [27].

vi) Proposed Classification Model using NAG with EfficientNet B0

A pre-trained network may be retrained to perform a different job using a process known as transfer learning (TL). A person's ability to apply their talents to a wide range of contexts gave rise to the idea. Creating a deep learning model for one job and then fine-tuning it such that just the essential alterations are made allows for efficient reuse for another activity. When it comes to TL, the new dataset is often quite similar to the old one; for example, both are image datasets. To that end, the fresh dataset often dictates the fine-tuning method employed on a pre-trained model [26].

To eliminate the excessive oscillations caused by momentum-based gradient descent, one may use NAG, which is also called nesterov accelerated gradient descent. Because momentum-based gradient descent may lead to model overfitting, the likelihood of a graph escaping the minima valley is lower [9].

An method that use convolutional neural networks is EfficientNet. The design of EfficientNet prioritizes both the accuracy and efficiency of models. Eight separate models ranging from B0 to B7 make up EfficientNet. The model's scales are based on three independent parameters. Resolution, breadth, and depth are these criteria. The width parameter indicates the total number of neurons in a layer, whereas the depth parameter quantifies the depth of the network. The resolution parameter indicates the granularity of the dataset that will be used to train the model. In contrast to current CNN models, which use a new activation function called Swish instead of a ReLU activation function, EfficientNet was used for classification in this work. In other state-of-the-art models, EfficientNet yields more efficient results by uniformly scaling depth, breadth, and resolution when the model is shrunk. Finding a grid to help determine the link between the baseline network's multiple scaling dimensions while dealing with a fixed resource restriction is the first step in the compound scaling technique. As a result, the parameters for depth, breadth, and resolution are scaled appropriately. Scaling the baseline network to the target network of choice is then accomplished by applying the coefficients [10].

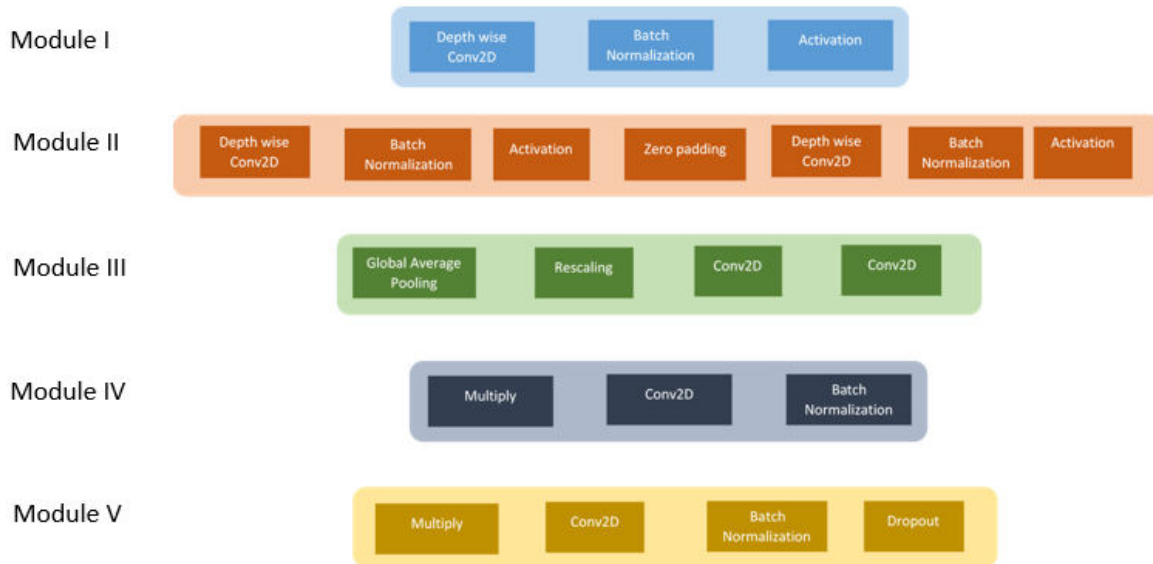


Figure5. Architecture of modules

In addition to EfficientNet-b0, another pretrained neural network has been used for image categorization. The core model of this team, EfficientNet-b0, uses input images with dimensions of 224×224 pixels. Mobile inverted bottleneck convolution (MBConv) is an implementation of EfficientNet-b0 that is comparable to MobileNetV2 but somewhat larger due to a greater FLOPS budget. By reducing parameter size and FLOPS by an order of magnitude, models based on EfficientNet are often recognized for their superior accuracy and efficiency compared to current state-of-the-art CNN models. Instead of using ReLU, which is used by other CNN models, EfficientNet models utilize Swish, which is a combination of a sigmoid and a linear activation function. In addition, EfficientNet-B0 uses the inverted residual block, which drastically decreases the amount of trainable parameters [14]. In Figure 6, we can see the EfficientNet-b0 design.

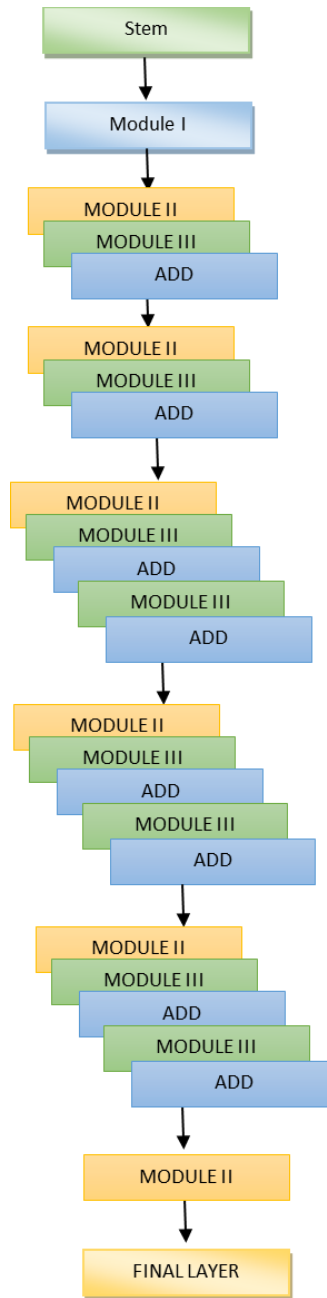


Figure 6. EFFICIENTNET B0 architecture

DepthwiseConv 2d

Deep learning architectures often use Depthwise Convolutional 2D (Depthwise Conv2D) to handle 2D input, such as images. Its lower computing cost in comparison to conventional convolutional layers makes it a preferred choice for embedded and mobile applications.

Batch Normalization

To ensure that each layer's inputs are normalized in a mini-batch, deep neural networks use batch normalization. By maintaining a consistent input distribution to each layer, it aids in fixing typical training issues like bursting or disappearing gradients. Training becomes quicker and generalization becomes better as a result of this stability.

Activation

Each neuron in a layer of a neural network has its output multiplied by a mathematical operation called an activation function. By introducing non-linearities into the network, activation functions enable neural networks to learn detailed patterns from input and approximate complex functions. (In this case, signoid is used.)

Zeropadding

Convolutional neural networks (CNNs) use zero-padding as a pre-convolutional procedure to resize the input volume. Increasing the input volume's spatial dimensions is achieved by surrounding its boundary with rows and columns of zeros..

Global Average Pooling

Convolutional neural networks (CNNs) often use the Global Average Pooling (GAP) method. This is especially true with CNN designs such as efficientnet, Google's Inception, and the widely used ResNet series. In the latter stages of a network, it is often used instead of completely linked layers, especially for image classification and other similar tasks.

Rescaling

To train a neural network more efficiently and with less instability, rescaling is a common technique in deep learning. It involves changing the size or distribution of the input data. Due to their sensitivity to the size and dispersion of input information, deep neural networks often need scaling. Suboptimal performance, sluggish convergence, and disappearing or expanding gradients are all possible outcomes of Improper scaling.

Algorithm – EfficientNetb0

- Using a compound coefficient, EfficientNet consistently scales all dimensions of depth, breadth, and resolution. It is a convolutional neural network design and scaling approach. The EfficientNet scaling approach uses a predetermined set of scaling coefficients to consistently scale the network width, depth, and resolution, as opposed to the traditional practice of arbitrarily scaling these elements. For principled, consistent scaling of network breadth, depth, and resolution, EfficientNet employs a compound coefficient technique.
- To enlarge the network's receptive field and catch more fine-grained patterns on a larger input image, additional layers are needed. This understanding justifies the use of the compound scaling approach.
- Squeeze-and-excitation blocks and the inverted bottleneck residual blocks from MobileNetV2 form the basis of the EfficientNet-B0 network.

Types of dental disease**Primary Endo with secondary Perio**

"Primary endo with secondary perio" is a term used in dentistry to describe a condition where the primary issue affecting a tooth is related to endodontic (inside the tooth) problems, while secondary issues involve periodontal (around the tooth) concerns.

Primary Perio with secondary Endo

"Primary perio with secondary endo" is a dental term used to describe a condition where the primary issue affecting a tooth is related to periodontal (around the tooth) problems, while secondary issues involve endodontic (inside the tooth) concerns.

Primary Endodontic Lesion

In dentistry, a "primary endodontic lesion" describes a situation where issues with the pulp and root canal system are the main concerns influencing a tooth.

Primary Periodontal Lesion

As a dentist, you may hear the term "primary periodontal lesion" used to describe a situation in which troubles with the gums and supporting bone are the main concerns impacting the tooth.

True combination Lesion

In dentistry, a "true combination lesion" is a situation where problems with the tooth's inner (the endodontic) and its surrounding (the periodontal) areas are present at the same time and contribute to the tooth's overall pathology.

Such situations include a combination of issues stemming from the tooth's internal and external structures, creating a challenging clinical situation that calls for thorough evaluation and treatment planning.

vii) Results

Accuracy—As a ratio of the number of observations that were accurately predicted to the total number of observations, accuracy is the most intuitive performance metric [25].

$$Accuracy = (TP + TN)/(TP + FP + FN + TN) \quad (2)$$

Precision—The total number of positive observations that were accurately predicted relative to the total number of positive observations expected is called precision.

$$Precision = TP/TP + FP \quad (3)$$

Recall (Sensitivity)—Recall is the ratio of correctly predicted positive observations to the all observations in actual class.

$$Recall = TP/TP + FN \quad (4)$$

F1 score— Precision and Recall are weighted to get this number. So, this number accounts for both false negatives and false positives outcomes.

$$F1\ Score = 2 * (Precision * Recall) / (Precision + Recall) \quad (5)$$

Specificity—The specificity (SP) of a prediction model is determined by dividing the total number of negative predictions by the number of negatives [25].

$$Specificity = TN/TN + FP \quad (6)$$

"Area under the ROC curve," a statistic that uses the ROC diagram as a two-dimensional square to quantify the area under the curve, is used to evaluate the model's quality when utilizing the ROC curve.

$$AUC = \int_0^1 \frac{TP}{p} d \frac{FP}{n} = \frac{1}{PN} \int_0^N TP dFP \quad (7)$$

- The first case, True Positive (TP), occurs when the classifier predicts that an image with a Caries label has Caries.
- The second case, False Positive (FP), occurs when the classifier predicts that an image with no Caries label has Caries.
- The third case, False Negative (FN), is when the classifier predicts an image with a Caries label as no Caries.
- The fourth case, called True Negative (TN), is when an image known to have no Caries label is predicted as no Caries by the classifier.

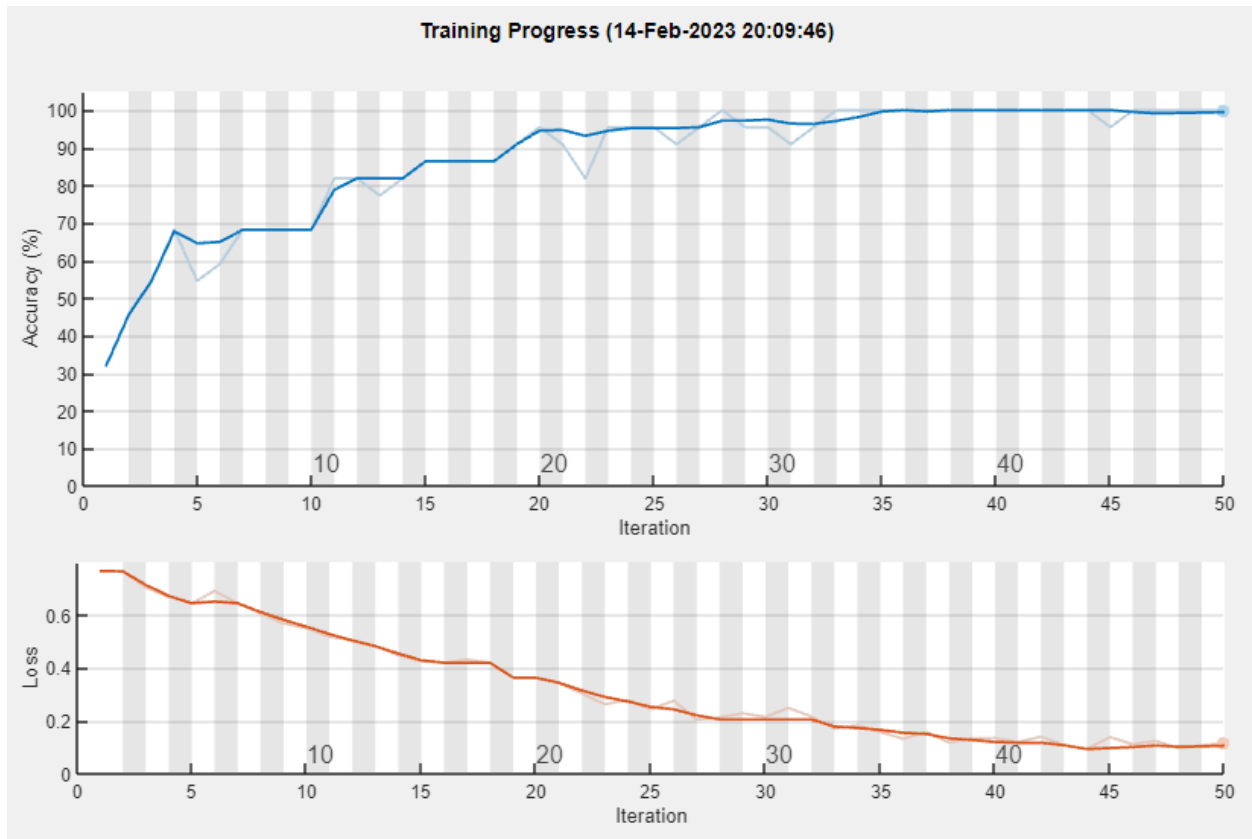


Figure7. TRAINNG MODEL

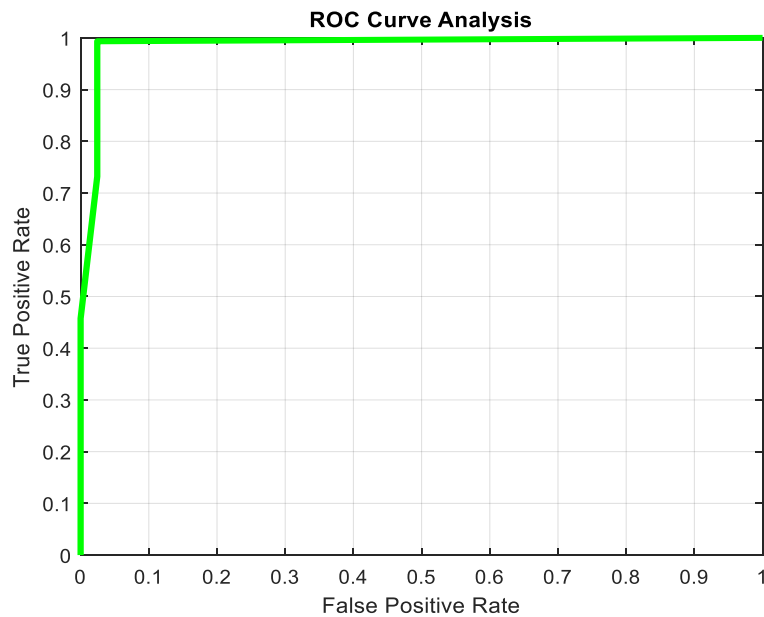


Figure8. ROC curve

Confusion Matrix: The tabular breakdown provided by the confusion matrix provides thorough insights into the sorts of errors in the model. True positives are forecasts for the positively

predicted class, true negatives are predictions for the negatively projected class, and false positives and false negatives are predictions for the incorrectly predicted classes, respectively. In binary classification tasks in particular, this matrix helps to identify the model's strengths and weaknesses by showing how well it distinguishes between classes [13]. Below is the figure displaying the confusion matrix.

Table1. Confusion matrix of the proposed model

CLASS	TP	FN	FP	TN
Class I	36	3	1	9
Class II	34	3	0	10
Class III	35	2	1	9
Class IV	11	1	1	4
Class V	34	1	2	8

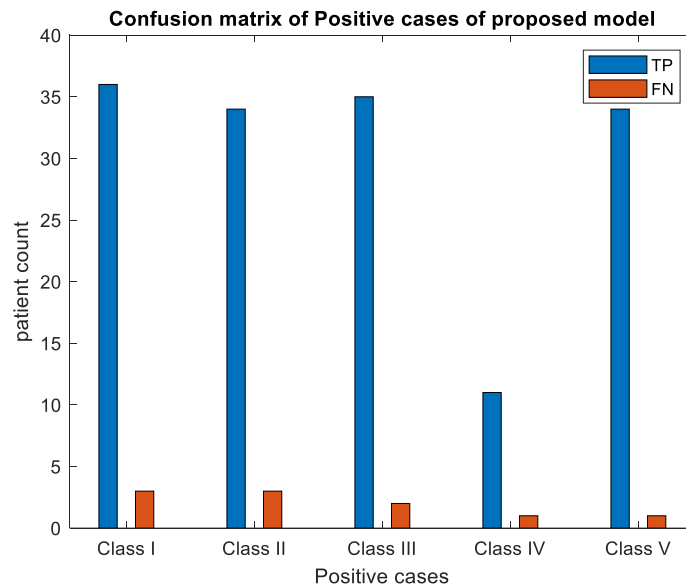


Figure9. Plots of positive cases

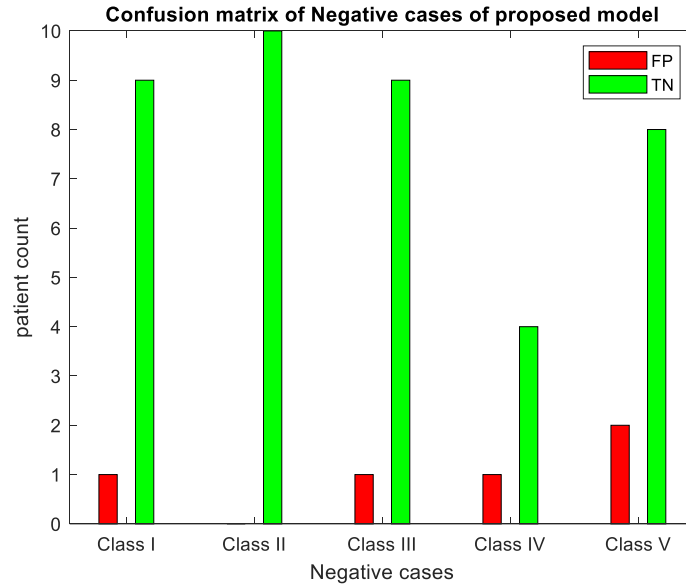


Figure10. Plots of positive cases

The confusion matrix of the suggested model, which describes how well it classified occurrences into five distinct classes, is shown in Tables 1, Figures 9, and 10. In Class I, the model rejected 9 cases (true negatives) properly, correctly recognised 36 instances (true positives), and erroneously categorised 3 instances (false negatives). It also mistakenly identified 1 instance as Class I (false positive). 34 true positives, 3 false negatives, 0 false positives, and 10 true negatives were found for Class II. 35 true positives, 2 false negatives, 1 false positive, and 9 true negatives are shown for Class III. There are 11 true positives, 1 false negative, 1 false positive, and 4 true negatives in Class IV, which includes less data points. Finally, 34 true positives, 1 false negative, 2 false positives, and 8 true negatives were obtained by the model for Class V. This matrix offers a thorough summary of the model's accuracy and the many mistakes it makes in each class.

Table2. Validation of the proposed model

CLASS	Precision	Sensitivity	Fscore	Specificity
Class I	97.30	92.31	94.74	90.00
Class II	100.00	91.89	95.77	100.00
Class III	97.22	94.59	95.89	90.00
Class IV	91.67	91.67	91.67	80.00
Class V	94.44	97.14	95.77	80.00

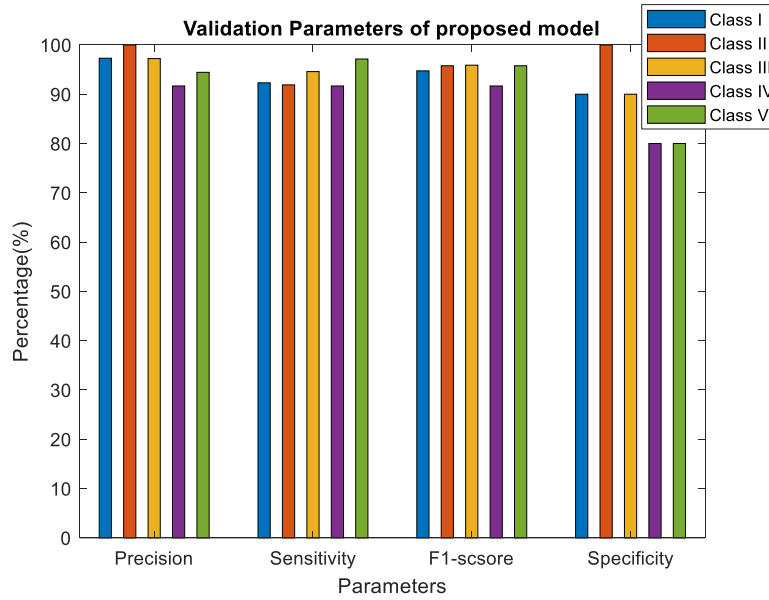


Figure 11. Validation of the proposed model

The suggested model's validation metrics are shown in Table 2, which demonstrates excellent performance across five classes. Class I has an F-score of 94.74%, a specificity of 90.00%, sensitivity of 92.31%, and precision of 97.30%. Class II attains 100.00% specificity, 91.89% sensitivity, 100.00% precision, and 95.77% F-score. 97.22% precision, 94.59% sensitivity, 95.89% F-score, and 90.00% specificity are recorded by Class III. Class IV has balanced measurements, including 80.00% specificity and 91.67% for F-score, sensitivity, and accuracy. Class V has 80.00% specificity, 95.77% F-score, 97.14% sensitivity, and 94.44% accuracy. Figure 11 shows these data, which show how good the model is in terms of accuracy, sensitivity, and F-score; nevertheless, specificity fluctuates more than other parameters.

Table3. Validation of the proposed model

CLASS	Accuracy
Class I	91.84
Class II	93.62
Class III	93.62
Class IV	88.24
Class V	93.33

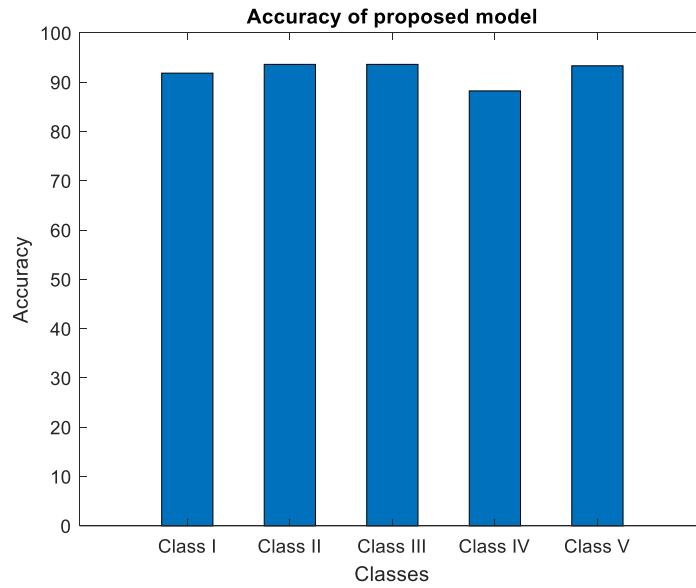


Figure 12. Validation of the proposed model

The accuracy of the suggested model is shown for five distinct classes in Table 3. Class I performs reliably, with an accuracy of 91.84%. Both Class II and Class III exhibit excellent accuracy levels of 93.62%, indicating a stable performance in categorization. Class IV's accuracy of 88.24% is somewhat lower, indicating some difficulties with accurate categorization. Class V continues to perform well, with 93.33% accuracy. With very slight variances in performance, these accuracy metrics—shown in Figure 12—highlight the model's general efficacy across the majority of classes.

Table4. Confusion matrix of the proposed and existing model

Methodology	TP	FN	FP	TN
PNN	129	31	20	25
RNN	132	28	16	29
LSTM	135	25	14	31
CNN	139	21	10	35
Proposed model	150	10	5	40

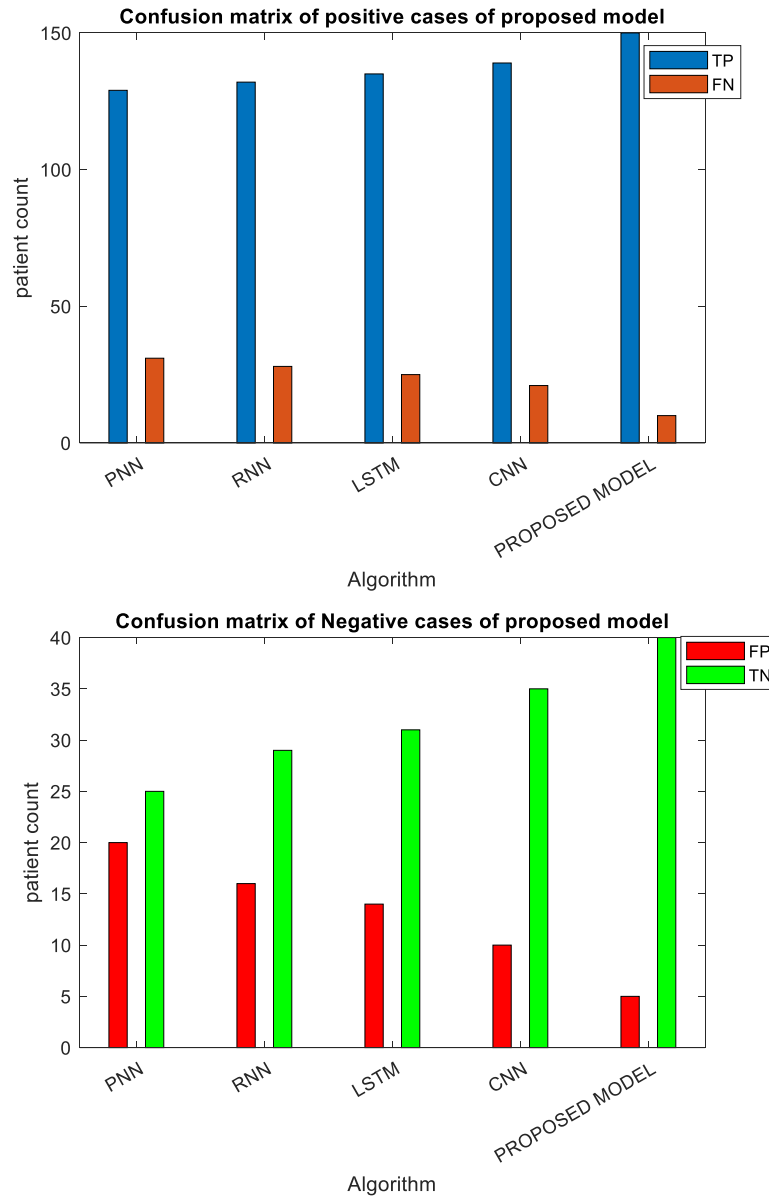


Figure13. Plots of positive and negative cases

PNN, RNN, LSTM, CNN, and the proposed model's confusion matrices are contrasted with those of the other four models in Table 4. With 150 true positives (TP), the lowest false negatives (FN) at 10, the lowest false positives (FP) at 5, and the greatest true negatives (TN) at 40, the suggested model performs better than the others. CNN comes next with 21 FN, 10 FP, 35 TN, and 139 TP. 135 TP, 25 FN, 14 FP, and 31 TN are recorded by LSTM. PNN performs the worst, with 129 TP, 31 FN, 20 FP, and 25 TN, while RNN displays 132 TP, 28 FN, 16 FP, and 29 TN. These outcomes, which are shown in Figure 13, demonstrate how well the suggested model can discriminate between positive and negative situations.

Table5. Comparison with Existing models

Methodology	Precision	Sensitivity	Fscore	Specificity
PNN	86.58	80.63	83.50	55.56
RNN	89.19	82.50	85.71	64.44
LSTM	90.60	84.38	87.38	68.89
CNN	93.29	86.88	89.97	77.78
Proposed model	96.77	93.75	95.24	88.89

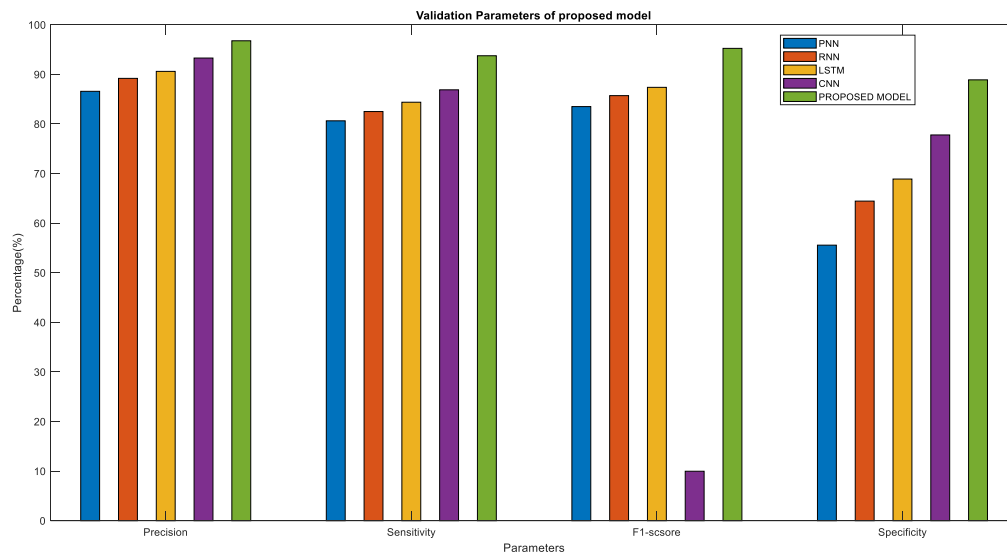


Figure14. Comparison with Existing models

In Table 4, the confusion matrices of the proposed model are compared to those of four other models that are already in existence: PNN, RNN, LSTM, and CNN. A total of 150 true positives (TP) and the lowest number of false negatives (FN) at 10, false positives (FP) at 5, and the largest number of true negatives (TN) at 40 are all characteristics of the suggested model, which outperforms the other models. After that comes CNN with 139 total points, 21 foreign points, 10 false positives, and 35 total points. A total of 135 TP, 25 FN, 14 FP, and 31 TN are recorded by LSTM. The performance of RNN is the highest, with 132 TP, 28 FN, 16 FP, and 29 TN, while the performance of PNN is the lowest, with 129 TP, 31 FN, 20 FP, and 25 TN. The visual representation of these findings, which can be seen in Figure 14, demonstrates that the suggested model is very accurate in discriminating between positive and negative situations.

Table 6. Accuracy comparison of proposed and existing model

Methodology	Accuracy
PNN	75.12
RNN	78.54
LSTM	80.98
CNN	84.88
Proposed model	92.68

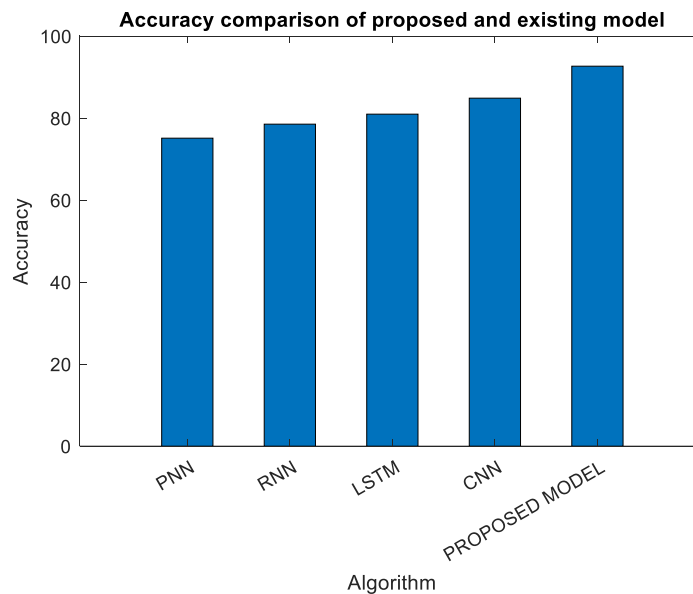


Figure 15. Accuracy comparison of proposed and existing model

The accuracy of the proposed model is evaluated in contrast to that of four other models that are already in existence. These models are the PNN, RNN, LSTM, and CNN models. The results of this evaluation are reported. The recommended model achieves the highest level of accuracy, which is 92.68%, when compared to other models such as PNN (75.12%), RNN (78.54%), LSTM (80.98%), and CNN (84.88%). Given this accomplishment, it can be deduced that the model that was suggested has a higher overall performance. Clearly, this demonstrates that the model that was provided is effective in correctly detecting instances over the whole of the dataset. Figure 15 provides a graphical representation of all of these accuracy comparisons, which makes it plainly clear that the proposed model has a significant performance advantage over the alternatives that are presently being used.

IV. CONCLUSION

By maintaining proper dental hygiene and staying away from sugary and acidic foods and beverages, you may protect your teeth against cavities, caries, and wear and tear. Traditional image segmentation algorithms may be painful to work with when dealing with complex dental X-ray images due to their slow processing times and inaccurate segmentation. To classify dental images for caries detection, this research employed Nesterov Accelerated Gradient (NAG)

optimization using EfficientNet-B0. In this paper, we provide a new hybrid ANN-UNN method for dental image segmentation. With an improved performance and a greater degree of accuracy of 92.68%, our suggested technique stands out from the competition. We may improve upon these outcomes in the future by combining other optimization strategies with further transfer learning.

REFERENCE

1. Oztekin, F., Katar, O., Sadak, F., Yildirim, M., Cakar, H., Aydogan, M., ...& Acharya, U. R. (2023). An explainable deep learning model to prediction dental caries using panoramic radiograph images. *Diagnostics*, 13(2), 226.
2. Tareq, A., Faisal, M. I., Islam, M. S., Rafa, N. S., Chowdhury, T., Ahmed, S., ...& Dudley, J. (2023). Visual diagnostics of dental caries through deep learning of non-standardised image graphs using a hybrid YOLO ensemble and transfer learning model. *International Journal of Environmental Research and Public Health*, 20(7), 5351.
3. Mao, Y. C., Chen, T. Y., Chou, H. S., Lin, S. Y., Liu, S. Y., Chen, Y. A., ... & Chiang, W. Y. (2021). Caries and restoration detection using bitewing film based on transfer learning with CNNs. *Sensors*, 21(13), 4613.
4. AHIRRAO, T. U., & BHAVE, R. (2023). A Novel Approach for Dental Caries Classification Using Transfer Learning.
5. Salunke, D., Mane, D., Joshi, R., & Peddi, P. (2022). Customized convolutional neural network to detect dental caries from radiovisiography (RVG) images. *International Journal of Advanced Technology and Engineering Exploration*, 9(91), 827-838.
6. Haghanifar, A., Majdabadi, M. M., & Ko, S. B. (2020). Paxnet: Dental caries detection in panoramic x-ray using ensemble transfer learning and capsule classifier. *arXiv preprint arXiv:2012.13666*.
7. Prajapati, S. A., Nagaraj, R., & Mitra, S. (2017, August). Classification of dental diseases using CNN and transfer learning. In *2017 5th International Symposium on Computational and Business Intelligence (ISCBI)* (pp. 70-74). IEEE.
8. Harsh, P., Chakraborty, R., Tripathi, S., & Sharma, K. (2021, June). Attention U-Net architecture for dental image segmentation. In *2021 International Conference on Intelligent Technologies (CONIT)* (pp. 1-5). IEEE.
9. Gaddam, D. K. R., Ansari, M. D., Vuppala, S., Gunjan, V. K., & Sati, M. M. (2022). A performance comparison of optimization algorithms on a generated dataset. In *ICDSMLA 2020: Proceedings of the 2nd International Conference on Data Science, Machine Learning and Applications* (pp. 1407-1415). Springer Singapore.
10. Dayı, B., Üzen, H., Çiçek, İ. B., & Duman, Ş. B. (2023). A novel deep learning-based approach for segmentation of different type caries lesions on panoramic radiographs. *Diagnostics*, 13(2), 202.
11. Kandel, I., Castelli, M., & Popovič, A. (2020). Comparative study of first order optimizers for image classification using convolutional neural networks on histopathology images. *Journal of imaging*, 6(9), 92.
12. Chen, I. D. S., Yang, C. M., Chen, M. J., Chen, M. C., Weng, R. M., & Yeh, C. H. (2023). Deep learning-based recognition of periodontitis and dental caries in dental x-ray images. *Bioengineering*, 10(8), 911.

13. Albalawi, E., Thakur, A., Ramakrishna, M. T., Bhatia Khan, S., SankaraNarayanan, S., Almarri, B., & Hadi, T. H. (2024). Oral squamous cell carcinoma detection using EfficientNet on histopathological images. *Frontiers in Medicine*, *10*, 1349336.
14. Deepak, G. D., & Krishna Bhat, S. (2024). Optimization of deep neural networks for multiclassification of dental X-rays using transfer learning. *Computer Methods in Biomechanics and Biomedical Engineering: Imaging & Visualization*, *12*(1), 2272976.
15. Meem, F. A., Ferdus, J., Sarkar, W. A., Ahmed, M. I., & Islam, M. S. (2023, May). Detection of Dental Issues Using the Transfer Learning Methods. In *Proceedings of the Fourth International Conference on Trends in Computational and Cognitive Engineering: TCCE 2022* (pp. 367-379). Singapore: Springer Nature Singapore.
16. Liyanage, V., Tao, M., Park, J. S., Wang, K. N., & Azimi, S. (2023). Malignant and non-malignant oral lesions classification and diagnosis with deep neural networks. *Journal of Dentistry*, *137*, 104657.
17. Ong, S. H., Kim, H., Song, J. S., Shin, T. J., Hyun, H. K., Jang, K. T., & Kim, Y. J. (2024). Fully automated deep learning approach to dental development assessment in panoramic radiographs. *BMC Oral Health*, *24*(1), 426.
18. Soni, A., Sethy, P. K., Dewangan, A. K., Nanthaamornphong, A., Behera, S. K., & Devi, B. (2024). Enhancing oral squamous cell carcinoma detection: a novel approach using improved EfficientNet architecture. *BMC Oral Health*, *24*(1), 601.
19. Elshamy, R., Abu-Elnasr, O., Elhoseny, M., & Elmougy, S. (2023). Improving the efficiency of RMSProp optimizer by utilizing Nesterov in deep learning. *Scientific Reports*, *13*(1), 8814.
20. Milani, O. H., Atici, S. F., Allareddy, V., Ramachandran, V., Ansari, R., Cetin, A. E., & Elnagar, M. H. (2024). A fully automated classification of third molar development stages using deep learning. *Scientific Reports*, *14*(1), 13082.
21. Lopez-Betancur, D., González-Ramírez, E., Guerrero-Mendez, C., Saucedo-Anaya, T., Rivera, M. M., Olmos-Trujillo, E., & Gomez Jimenez, S. (2024). Evaluation of Optimization Algorithms for Measurement of Suspended Solids. *Water*, *16*(13), 1761.
22. Fernandez, K., & Chang, C. (2012). Teeth/palate and interdental segmentation using artificial neural networks. In *Artificial Neural Networks in Pattern Recognition: 5th INNS IAPR TC 3 GIRPR Workshop, ANNPR 2012, Trento, Italy, September 17-19, 2012. Proceedings 5* (pp. 175-185). Springer Berlin Heidelberg.
23. Lin, S. Y., & Chang, H. Y. (2021). Tooth numbering and condition recognition on dental panoramic radiograph images using CNNs. *IEEE Access*, *9*, 166008-166026.
24. Moghaddam, M. J., & Soltanian-Zadeh, H. (2011). Medical image segmentation using artificial neural networks. *Artificial neural networks-Methodological advances and biomedical applications*, 121-138.
25. Sivagami, S., Chitra, P., Kailash, G. S. R., & Muralidharan, S. R. (2020, August). Unet architecture based dental panoramic image segmentation. In *2020 International Conference on Wireless Communications Signal Processing and Networking (WiSPNET)* (pp. 187-191). IEEE.
26. Ching, W. P., Abdullah, S. S., Shapiai, M. I., & Islam, A. M. (2024). Transfer Learning for Alzheimer's Disease Diagnosis Using EfficientNet-B0 Convolutional Neural Network. *Journal of Advanced Research in Applied Sciences and Engineering Technology*, *35*(1), 181-191.

27. Jusman, Y., Tamarena, R. I., Puspita, S., Saleh, E., & Kanafiah, S. N. A. M. (2020, August). Analysis of features extraction performance to differentiate of dental caries types using gray level co-occurrence matrix algorithm. In *2020 10th IEEE International Conference on Control System, Computing and Engineering (ICCSCCE)* (pp. 148-152). IEEE.